

Article

# Synthesis and Characterization of Magnetic Nanoparticles (MNP) and MNP-Chitosan Composites

Monica Namizie Asey<sup>1,2</sup>, Norhaizan Mohd Esa<sup>3</sup>, Che Azurhanim Che Abdullah<sup>1,a,2</sup>

<sup>1</sup> Faculty of Science, Universiti Putra Malaysia (UPM), 43400 Serdang, Selangor, Malaysia  
E-mail: <sup>a</sup>azurhanim@upm.edu.my

<sup>2</sup> Material Synthesis and Characterization Laboratory, Institute of Advanced Technology, Universiti Putra Malaysia (UPM), 43400 Serdang, Selangor, Malaysia

<sup>3</sup> Department of Nutrition and Dietetics, Faculty of Medicine and Health Sciences, Universiti Putra Malaysia (UPM), 43400 Serdang, Selangor, Malaysia

**Abstract**— Coating of iron oxide nanoparticles (MNP) is the common approach to reduce the effects of direct toxicity due to the ion oxidation that lead to the damage of DNA. This study investigates the effect of different concentration of Chitosan (Cs) used to coat the magnetic nanoparticle with variation in the crystallite size, chemical bonding, changes in weight and surface morphology. From the XRD results, it shows that the sample 1MNP-1Cs has optimum size of  $13.42 \pm 0.01$  nm. From the FTIR analysis, it is revealed that there are three types of chemical bonding that occur in the MNP-Cs composites which are stretching vibrations of C-H, N-H vibration belonging to Cs and the Fe-O bonds from the MNP. From the FESEM analysis, it is found that the MNP-Cs composites have a well-shaped with spherical in form, as well as, smooth surfaces. As for TGA, the thermal decomposition of MNP nanocomposites was based on the amount of Cs and MNP used to produce the nanocomposites. Further studies will be conducted to find the optimum ratio of MNP-Cs for anticancer drug delivery application.

**Keywords**— Iron oxide; Chitosan; Nanotechnology; Composites; Superparamagnetism.

## I. INTRODUCTION

Magnetic nanoparticles (MNP) are nanoparticles that easily manipulated by using magnetic fields. The most studied MNP nowadays is Ferrite nanoparticle. When the Ferrite particles size is less than 76 nm it become superparamagnetic [1]. Hence preventing self-agglomeration because it can only show their magnetism when magnetic field is introduced to it. When the magnetic field is detached from it, the remanence goes back to zero. Research conducted previously by Tran et al. (2010) showed that the magnetic nanoparticles (MNP) was simply disjointed during the material preparation due to its magnetic properties and makes them suitable for drug delivery, hyperthermia treatment for cancer and many other applications [2].

Chitosan (Cs) is a linear polysaccharide containing randomly distributed b-(1-4)-linked D-glucosamine and N-acetyl-D-glucosamine. It is one of the main cationic polymers and the second most plentiful polysaccharides found in nature. It is broadly used in the field of biomedical and the industrial fields [3]. The primary amine groups of Cs offer unique properties to Cs make it applicable for further functionalization with specific components, such as various drugs, specific binding site or other functional groups [4]. Thus, due to its cationic nature of chitosan, it allows the ionic cross linking between Cs and multivalent anions, and could

be the appropriate type of polymer that can be treated to modify the iron oxide nanoparticles.

Research conducted previously by Ankamwar et al. (2010) showed that MNP toxicity occurs through multiple mechanisms, limiting the functionality of these materials in tissue engineering applications [5]. Surface modification achieved via coating of iron oxide nanoparticles is the common approach applied to reduce the effects of direct toxicity. So in order to reduce the toxicity, the MNP will be coated with polysaccharides of interest which is Cs at different ratios. Thus, the first objective of this project is to synthesize the magnetic nanoparticles (MNP) using co-precipitation method. The second objective is to conjugate the synthesized MNP using Cs then characterizes the MNP and MNP-Cs composites by using X-ray diffraction (XRD), Fourier Transform Infrared Spectroscopy (FTIR), thermal gravimetric analysis (TGA), and Field Emission Scanning Electron Microscopy (FESEM). The third objective is to investigate the effects of different ratio of MNP and Cs used in producing MNP-Cs composites by using XRD, FTIR, FESEM and TGA.

## II. EXPERIMENTAL

### A. Chemicals and Materials

Ferric chloride ( $\text{FeCl}_3 \cdot 6\text{H}_2\text{O}$ , 99 %), ferrous chloride ( $\text{FeCl}_2 \cdot 4\text{H}_2\text{O}$ , 98 %), aqueous ammonia ( $\text{NH}_4\text{OH}$ , 28 %), Chitosan deacetylated ( $\text{C}_{56}\text{H}_{103}\text{N}_9\text{O}_{39}$ , 75-85 %), aqueous acetic acid ( $\text{CH}_3\text{COOH}$ , 99.8 %) and deionized water.

### B. Instruments

The characterization of MNP-Cs composites was carried out by the means of X-ray diffraction (XRD) (X'pert Pro, PANalytical Philips, The Netherlands), Fourier Transform infrared spectroscopy (FTIR) (Thermo Nicolet, Nicolet 6700), and Thermalgravimetric Analysis (TGA) (TGA/DSC 1 HT, Mettler Toledo, Schweiz). The surface morphology of the nanocomposite was determined using Field Emission Scanning Electron Microscope (FESEM/ Fei,Nova Nanosem 230).

### C. Synthesis of $\text{Fe}_3\text{O}_4$ Magnetic Nanoparticles

The superparamagnetic  $\text{Fe}_3\text{O}_4$  nanoparticles, were prepared by chemical co-precipitation method. Typically, ferric trichloride hexahydrate and ferrous chloride tetrahydrate were mixed in 150 mL of deionized water with a molar ratio of 2:1 and stirred and heated to 80 °C until the appearance of a dark orange color under the nitrogen gas flow. Then 20 mL of aqueous ammonia was dropwise added to the solution, and the mixture was stirred at 80 °C for 1 hour. After cooled to room temperature, the black precipitate was separated through centrifugation process at 6000 rpm for 10 min and washed thoroughly with deionized water three times. Finally, the product was dried in an oven at 60 °C.

### D. Preparation of MNP – Chitosan

Cs-coated magnetic iron oxide nanoparticles were synthesized through in situ co-precipitation method where  $\text{Fe}^{2+}$  and  $\text{Fe}^{3+}$  salts were precipitated in the presence of chitosan.

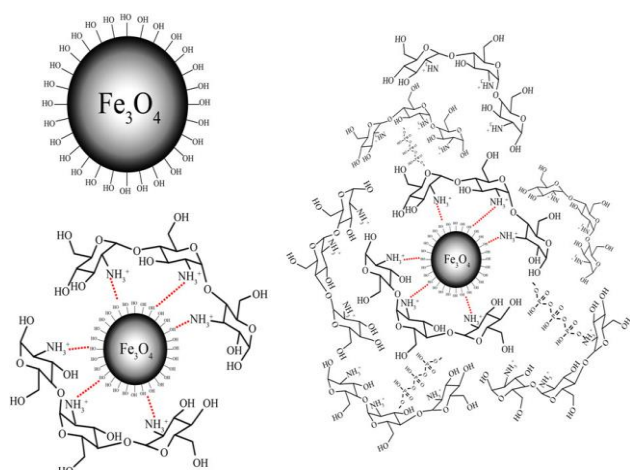


Fig. 1 Schema of in situ synthesized chitosan-coated magnetic nanoparticles (MNP-Cs) [6]

Cs (1 g) was dissolved in 100 mL deionized water which had been added with 0.5 mL of acetic acid stirred for 18 hours at 500 rpm and kept at 45 °C. 1g of Iron Oxide ( $\text{Fe}_3\text{O}_4$ ) were dissolved in 100 mL of deionized water and 100 mL chitosan solution by vigorously stirring at 800 rpm, at room

temperature for 18 hours. The colloidal Cs coated magnetic  $\text{Fe}_3\text{O}_4$  nanoparticles were extensively washed with deionized water and separated by magnetic decantation for several times (Fig. 1).

There are several ratios of MNP and Cs used in producing MNP-Cs composites in order to investigate the optimum concentration of MNP and Cs used in producing MNP- Cs composites mainly as shown in Table I.

TABLE I  
CONCENTRATION OF MNP AND CS USED IN PRODUCING MNP-  
CS COMPOSITES

Amount of MNP (g)	Amount of Chitosan powder use in producing Chitosan solution (g)	Final Product MNP-Cs composites concentration
1	0	1gMNP + 0 Cs
1	1	1g MNP + 1g Cs
2	1	2g MNP + 1g Cs
3	1	3g MNP + 1g Cs
1	0.5	1g MNP + 0.5g Cs
1	1.5	1g MNP + 1.5g Cs

## III.RESULTS AND DISCUSSION

### A. X-Ray Diffraction Analysis on MNP-Cs Composites

Fig. 2 shows the results of XRD analysis for MNP synthesized via co-precipitation method coated with Cs at different amount of Cs (0.5, 1.0 and 1.5 g). The MNP diffraction patterns have five main peaks at  $2\theta$  values of 30.4°, 35.8°, 43.5°, 57.5° and 63.2°. On the other hand, the 0.5 Cs-MNP, 1.5Cs-MNP, and 1Cs-MNP nanocomposite exhibited main peaks are 30.2°, 35.7°, 43.5°, 57.4°, and 62.9°.

XRD analysis for different amount of MNP concentration used to produce MNP-CS composites (1.0, 2.0 and 3.0 g) are presented in the Fig. 3. Similarly, for 2MNP-Cs and 3MNP-Cs the diffraction patterns at  $2\theta$  values is 30.4°, 35.8°, 43.5°, 57.5° and 63.2° while for 1MNP-Cs the peaks is at 30.2°, 35.7°, 43.5°, 57.4°, and 62.9° corresponding to the random orientation of the MNP from (220), (311), (400), (511), and (440) crystal planes. The positions and relative intensities for all the observed peaks follow the cubic crystalline system of  $\text{Fe}_3\text{O}_4$  nanoparticles (ICDD: 01-075-0449). The narrow shape peaks of the nanocomposites indicated that the nanoparticles have relatively high crystallinity. These findings are in agreement with the previously study reported by Mahdavi et al. [7].

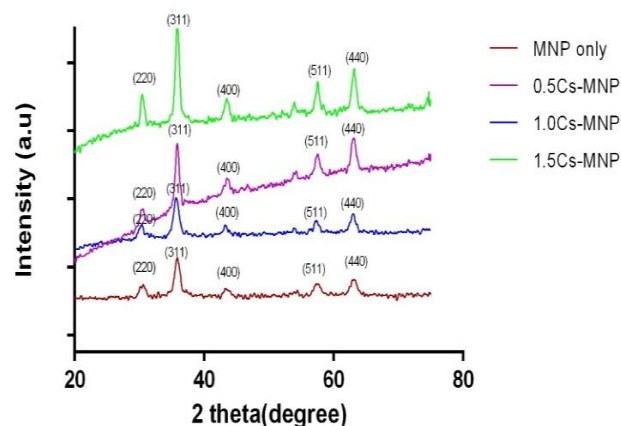


Fig. 2 XRD diffraction for MNP, 0.5Cs-MNP, 1.0Cs-MNP, and 1.5Cs-MNP at  $2\theta$  to 80°

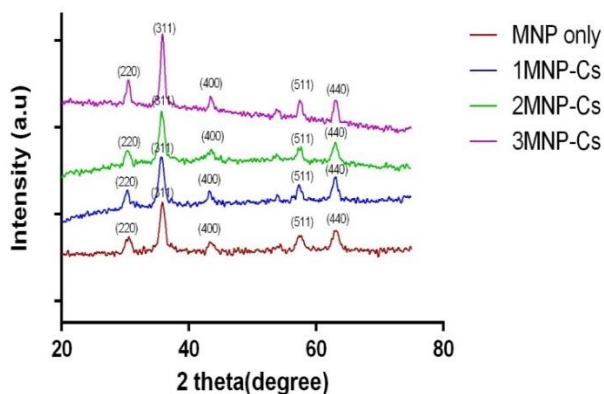


Fig. 3 XRD diffraction for MNP, 1MNP-Cs, 2MNP-Cs, and 3MNP-Cs at 20° to 80°

Broadness of the diffraction peaks was related to particle sizes. Scherrer's equation;

$$D = \frac{k\lambda}{\beta \cos\theta}$$

Where; D= Average particle size

K= Scherrer's Constant

= 0.94

$\lambda$  = Wavelength of X-Ray

= 1.54059 Å m

$\beta$  = FWHM (Full Width at Half Maximum)

Scherrer's equation was used to calculate the crystallite size D. The broadening of Bragg's peaks indicates the formation of nanoparticles. The calculated mean crystallite size of the MNP nanocomposites synthesized by co-precipitation method was presented in Table II.

TABLE II  
MEAN CRYSTALLITE SIZE OF 0.5 CS-MNP, 1CS-MNP, 1.5CS-MNP, 2MNP-CS AND 3MNP-CS

Type of samples	Mean crystallite size (nm)
0.5 Cs – MNP	29.85
1.0 Cs – MNP (1MNP-Cs)	13.42
1.5 Cs- MNP	16.79
2MNP – Cs	44.77
3MNP – Cs	20.66

Please note that 1.0Cs-MNP was named as 1.0 MNP-Cs in the case of different amount of MNP.

### B. Fourier Transform Infrared Spectroscopy

FTIR were performed on both different MNP and Cs concentrations to produce MNP-Cs nanocomposites in order to study the chemical bonding of the sample.

*FTIR analysis on MNP-Cs composites for different Cs concentration:* FTIR was performed to further confirm the functional groups that exist in the synthesized materials. In the case of Cs coated MNP at different Cs concentration, the coating of Cs is established by the appearance of the band at 2350 cm<sup>-1</sup>, 2920 cm<sup>-1</sup> and 2340 cm<sup>-1</sup> for 0.5 Cs-MNP, 1.0 Cs-MNP, 1.5 Cs-MNP, respectively which are considered to be the stretching vibrations of C-H. The bands at 1620 cm<sup>-1</sup>, 1600 cm<sup>-1</sup> and 1610 cm<sup>-1</sup> for 0.5 Cs-MNP, 1.0 Cs-MNP, and 1.5 Cs-MNP are relevant to be the N-H vibration belonging to Cs [8]. In addition, the bands noticeable at 552

cm<sup>-1</sup> for 0.5 Cs-MNP, 567 cm<sup>-1</sup> for 1.0 Cs-MNP, and 557 cm<sup>-1</sup> for 1.5 Cs-MNP reveal the Fe-O bonds from the MNP (Fig. 4). The results obtained are in line with previous work carried out by Saeb et al. (2017) [9].

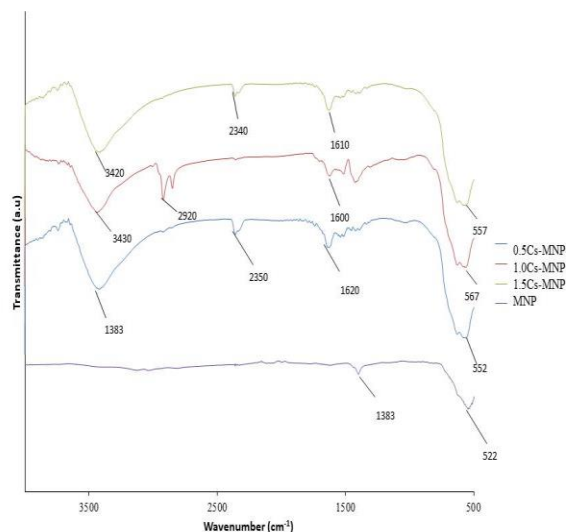


Fig. 4 The FTIR spectrum for 0.5 Cs-MNP, 1 Cs-MNP, 1.5 Cs-MNP and MNP at the range of 500-4000 cm<sup>-1</sup>

*FTIR analysis on MNP-Cs composites for different MNP concentration:* The coating of Cs for 1 MNP-Cs, 2 MNP-Cs, 3 MNP-Cs at different MNP concentration are established by the clear formation of the band observed at 2920 cm<sup>-1</sup>, 2910 cm<sup>-1</sup>, and 2340 cm<sup>-1</sup> respective to 1 MNP-Cs, 2 MNP-Cs, 3 MNP-Cs indicative of the C-H stretching vibrations in Cs. The bands at 1600 cm<sup>-1</sup>, 1590 cm<sup>-1</sup> and 1600 cm<sup>-1</sup> in accordance with 1 MNP-Cs, 2 MNP-Cs, 3 MNP-Cs signified the N-H vibration for the Cs (Fig. 5). Furthermore, the Fe-O bond can be seen at 567 cm<sup>-1</sup>, 542 cm<sup>-1</sup> and 534 cm<sup>-1</sup> for 1 MNP-Cs, 2 MNP-Cs, 3 MNP-Cs respectively as reported by Lasheen et al. (2016) [10].

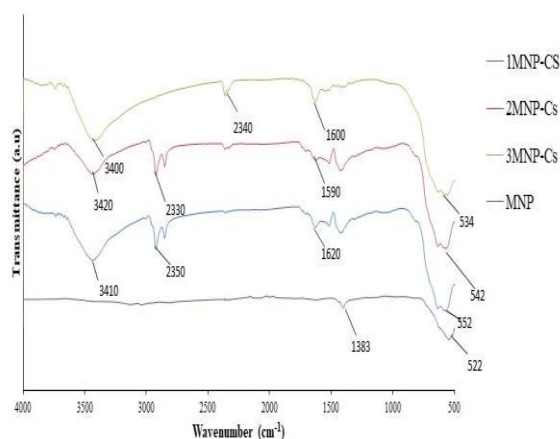


Fig. 5 The FTIR spectrum for 1 MNP-Cs, 2 MNP-Cs, 3 MNP-Cs and MNP at the range of 500-4000 cm<sup>-1</sup>

### C. Thermal Gravimetric Analysis

TGA was used to determine the weight percentage of Cs on the MNP surface. TGA measures weight changes in a

material as a function of temperature (or time) under a controlled atmosphere and in this analysis; the heating rate of  $10\text{ }^{\circ}\text{C min}^{-1}$  in a nitrogen atmosphere ( $50\text{--}800^{\circ}\text{C}$ ) was used.

*MNP-Cs composites for different Cs concentration:* Fig. 6 shows TGA performed on MNP-Cs composites for different Cs concentration. The initial weight loss for all samples can be explained by a loss of water molecules. Table III, IV and V showed the percentage weight loss according to the temperature. From the data, the nanocomposite has 3 steps of weight loss. The first weight loss revealed about the physical loss of hydrating water molecules which are about 2.41, 0.97, and 1.57 % for 0.5 Cs-MNP, 1.0 Cs-MNP, and 1.5 Cs-MNP respectively. Immediately after the decomposition of water molecule, Cs started to decompose. The nanocomposite with the most amount of Cs is determined to be 1.0 Cs-MNP (12.88 %) followed by 0.5 Cs-MNP (2.38 %) and the nanocomposite with the least amount of Cs is 1.5 Cs-MNP (1.72 %). The data obtained is supported by earlier work done by Rao et al. (2017) [11]. Finally, the last weight loss represents the changes in phase from  $\text{Fe}_3\text{O}_4$  to  $\text{FeO}$  as the TGA was conducted in the presence of nitrogen gas. Initially, the amount of MNP is the same, however after the Cs coating process, there is a reduction of the amount of MNP coated. The most amount of MNP is 2Cs-MNP (96.71 %), and the least is 1Cs-MNP (86.15 %).

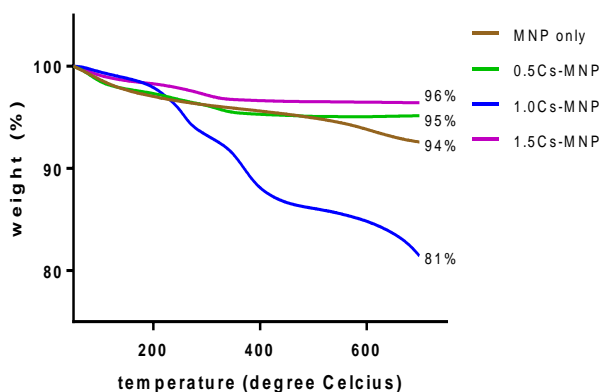


Fig. 6 TGA for magnetic iron oxide nanoparticles coated with Chitosan (Cs) at different Cs concentration ratio (0.5, 1.0 and 1.5)

TABLE III  
THE WEIGHT LOSS OF 0.5CS-MNP RELATIVE TO THE TEMPERATURE

Temperature ( $^{\circ}\text{C}$ )	Weight loss (%)
53-171	2.41
171-443	2.38
443-527	0.14
Residue (%)	95.07

TABLE IV  
THE WEIGHT LOSS OF 1 CS-MNP RELATIVE TO THE TEMPERATURE

Temperature ( $^{\circ}\text{C}$ )	Weight loss (%)
54-134	0.97
134-498	12.88
498-704	4.76
Residue (%)	81.39

TABLE V  
THE WEIGHT LOSS OF 1.5 CS-MNP RELATIVE TO THE TEMPERATURE

Temperature ( $^{\circ}\text{C}$ )	Weight loss (%)
53-177	1.57
177-369	1.72
369-514	0.18
Residue (%)	96.53

*MNP-Cs composites for different MNP concentration:* The percentage weight loss of 1 MNP-Cs, 2 MNP-Cs, 3 MNP-Cs were displayed in table VI, VII and VIII accordingly and Fig. 7. As stated previously, the first weight loss mainly due to the evaporation of water molecules which is about 0.97, 0.88, and 1.07 % for 1 MNP-Cs, 2 MNP-Cs, 3 MNP-Cs respectively [1]. Followed by the Cs decompositions about 12.88 % for 1 MNP-Cs, 13.26% for 2 MNP-Cs, and 2.35 % for 3 MNP-Cs. Therefore, it was discovered that the amount of Cs coating was affected by the amount of the MNP. As shown in Table IX, the third weight loss were due to the phase transition of  $\text{Fe}_3\text{O}_4$  to  $\text{FeO}$  so, the amount of MNP is about 86.15 %, 85.86%, and 96.58% 1 MNP-Cs, 2 MNP-Cs, 3 MNP-Cs accordingly.

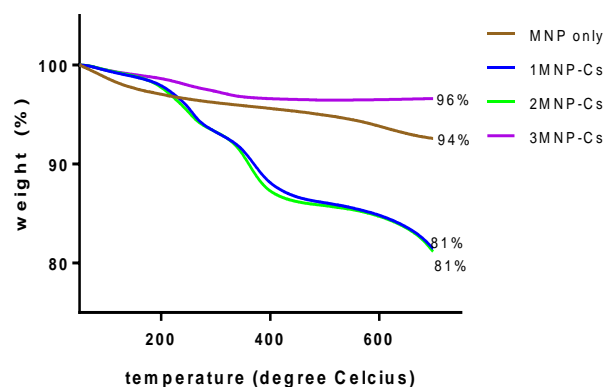


Fig. 7 TGA for magnetic iron oxide nanoparticles coated with Chitosan (Cs) at different MNP concentration ratio (1.0, 2.0 and 3.0)

TABLE VI  
THE WEIGHT LOSS OF 1 MNP-CS RELATIVE TO THE TEMPERATURE

Temperature ( $^{\circ}\text{C}$ )	Weight loss (%)
54-134	0.97
134-498	12.88
498-704	4.76
Residue (%)	81.39

TABLE VII  
THE WEIGHT LOSS OF 2 MNP-CS RELATIVE TO THE TEMPERATURE

Temperature ( $^{\circ}\text{C}$ )	Weight loss (%)
56-134	0.88
134-499	13.26
499-704	4.73
Residue (%)	81.13



TABLE VIII  
THE WEIGHT LOSS OF 3 MNP-CS RELATIVE TO THE TEMPERATURE

Temperature (°C)	Weight loss (%)
56-168	1.07
168-422	2.35
422-507	0.11
Residue (%)	96.47

TABLE IX  
THE WEIGHT LOSS OF BARE MNP RELATIVE TO THE TEMPERATURE

Temperature(°C)	Percentage weight loss (%)
62-136	1.82
136-298	1.67
298-603	2.43
Residue	94.08

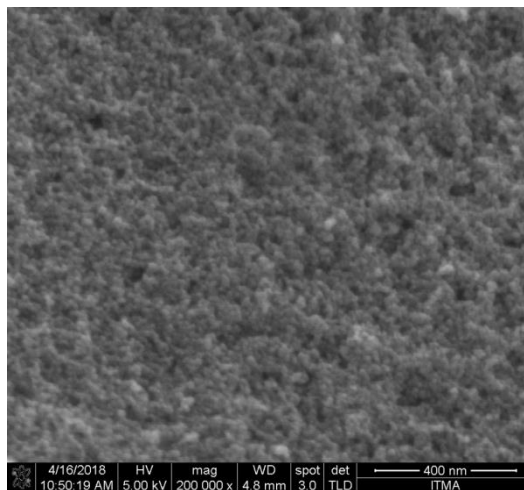


Fig. 10 The FESEM analysis for 3 MNP-Cs at 200 000x magnification

#### D. Field Emission Scanning Electron Microscopy

The morphology for the MNP–Cs composites for 0.5 Cs-MNP, 1 MNP-Cs and 3 MNP-Cs were shown in Fig. 8, 9 and 10. From Fig. 8, it is clear that  $\text{Fe}_3\text{O}_4$  nanoparticles bonded well with Cs and have well-shaped spherical form with smooth surfaces and there were no defects on the surface of MNP-Cs due to their compact structure and dense cross-linked biopolymer shells as reported by Ding et al. (2015)[12].

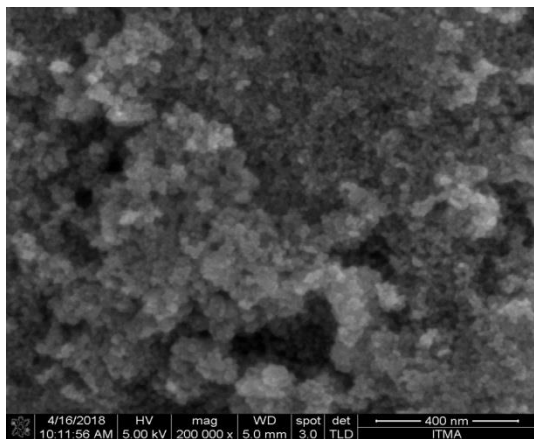


Fig. 8 The FESEM analysis for 0.5 Cs-MNP at 200 000x magnification

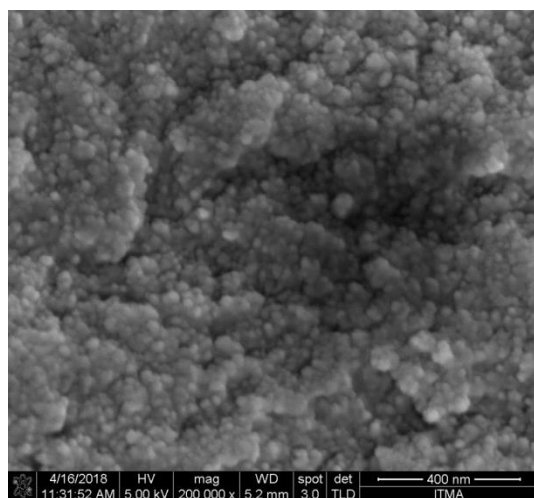


Fig. 9 The FESEM analysis for 1 Cs-MNP at 200 000x magnification

#### IV. CONCLUSIONS

MNP is a flexible material which can be used in many fields including biomedical field. The MNP used in this project is Iron Oxide coated with Cs. It was successfully synthesised by using the co-precipitation method. The mean crystallite size was identified by using XRD analysis. From the XRD results, we can conclude that when the size of the MNP is so small that it exceeded the critical size, superparamagnetism feature is attained.

The superparamagnetism characteristic is the most important for application in the biomedical field. From the FTIR analysis, it is revealed that there are three types of chemical bonding that occur in the MNP-Cs composites which are C-H stretching vibrations in Cs, N–H vibration for the Cs and Fe-O bond on MNP which confirm that the MNP were successfully coated with Cs. From the FESEM analysis, it is found that the MNP-Cs composites have a well-shaped spherical form with smooth surfaces and there were no defects detected. As for TGA, the thermal decomposition of MNP nanocomposites was affected by the amount of Cs and MNP.

#### ACKNOWLEDGMENT

This project manages to come to success thanks to the members of NANOTEDD group in Biophysics Lab, Physics Department and every personnel in the Electro-analysis Lab, Chemistry Department, UPM. This project also manages to come to success thanks to Ministry of Education for Fundamental Research Grant Scheme (UPM/FRGS/5524949), Universiti Putra Malaysia through Dana Tautan (DT-9200802).

#### REFERENCES

- [1] Q. Li, C. W. Kartikowati, S. Horie, T. Ogi, T. Iwaki, and K. Okuyama, "Correlation between particle size/domain structure and magnetic properties of highly crystalline  $\text{Fe}_3\text{O}_4$  nanoparticles," *Scientific Reports*, vol. 7(1), pp. 9894, 2017.
- [2] N. Tran, A. Mir, D. Mallik, A. Sinha, S. Nayar, and T. J. Webster, "Bactericidal effect of iron oxide nanoparticles on *Staphylococcus aureus*," *International Journal of Nanomedicine*, vol. 5, pp. 277, 2010.
- [3] C. Choi, J. P. Nam, and J. W. Nah, "Application of chitosan and chitosan derivatives as biomaterials," *Journal of Industrial and Engineering Chemistry*, vol. 33, pp. 1-10, 2016.
- [4] S. Agnihotri, S. Mukherji, and S. Mukherji, "Antimicrobial chitosan–PVA hydrogel as a nanoreactor and immobilizing matrix for silver nanoparticles," *Applied Nanoscience*, vol. 2(3), pp. 179-188, 2012.

- [5] B. Ankamwar, T. C. Lai, J. H. Huang, R. S. Liu, M. Hsiao, C. H. Chen, and Y. K. Hwu, "Biocompatibility of Fe<sub>3</sub>O<sub>4</sub> nanoparticles evaluated by in vitro cytotoxicity assays using normal, glia and breast cancer cells," *Nanotechnology*, vol. 21(7), pp. 075102, 2010.
- [6] G. Unsoy, S. Yalcin, R. Khodadust, G. Gunduz, and U. Gunduz, "Synthesis optimization and characterization of chitosan-coated iron oxide nanoparticles produced for biomedical applications," *Journal of Nanoparticle Research*, vol. 14(11), pp. 964, 2012.
- [7] M. Mahdavi, M. B. Ahmad, M. J. Haron, F. Namvar, B. Nadi, M. Z. A. Rahman, and J. Amin, "Synthesis, surface modification and characterisation of biocompatible magnetic iron oxide nanoparticles for biomedical applications," *Molecules*, vol. 18(7), pp. 7533-7548, 2013.
- [8] J. M. Shen, L. Xu, Y. Lu, H. M. Cao, Z. G. Xu, T. Chen, and H. X. Zhang, "Chitosan-based luminescent/magnetic hybrid nanogels for insulin delivery, cell imaging, and antidiabetic research of dietary supplements," *International Journal of Pharmaceutics*, vol. 427(2), pp. 400-409, 2012.
- [9] M. R. Saeb, M. Nonahal, H. Rastin, M. Shabaniyan, M. Ghaffari, G. Bahlakeh, and D. Puglia, "Calorimetric analysis and molecular dynamics simulation of cure kinetics of epoxy/chitosan-modified Fe<sub>3</sub>O<sub>4</sub> nanocomposites," *Progress in Organic Coatings*, vol. 112, pp. 176-186, 2017.
- [10] M. R. Lasheen, I. Y. El-Sherif, M. E. Tawfik, S. T. El-Wakeel, and M. F. El-Shahat, "Preparation and adsorption properties of nano magnetite chitosan films for heavy metal ions from aqueous solution," *Materials Research Bulletin*, vol. 80, pp. 344-350, 2016.
- [11] K. M. Rao, A. Kumar, and S. S. Han, "Polysaccharide-based magnetically responsive polyelectrolyte hydrogels for tissue engineering applications" *Journal of Materials Science & Technology*, vol. 34(8), pp. 1371-1377, 2018.
- [12] Y. Ding, S. Z. Shen, H. Sun, K. Sun, F. Liu, Y. Qi, and J. Yan, "Design and construction of polymerized-chitosan coated Fe<sub>3</sub>O<sub>4</sub> magnetic nanoparticles and its application for hydrophobic drug delivery," *Materials Science and Engineering: C*, vol. 48, pp. 487-498, 2015.